RESEARCH ARTICLE

Preparation of a novel non-burning polyaluminum chloride residue(PACR) compound filler and its phosphate removal mechanisms

Qiang Li[1] · Jingshen Zhang[1] · Jingqing Gao[1] · Zhenzhen Huang[2] · Haoxin Zhou[2] · Haoyu Duan[1] · Zihao Zhang[3]

Abstract

As an inevitable industrial by-product, polyaluminum chloride residue (PACR) will cause serious harm to the environment if directly buried and dumped. The aim of this paper was searched a new economical, environmental, and practical way of utilization for PACR. In this paper, a novel non-burning PACR compound filler was made from mainly PACR. The prepared compound filler has excellent physical properties and phosphate adsorption efficiency of up to 99.9%. Static adsorption experiments showed that the adsorption process of phosphorus by the compound filler conformed to the pseudo-second-order kinetic model and intra-particle diffusion model. Langmuir and Freundlich isotherm models described the phosphorus adsorption process well, and the maximum phosphate adsorption capacity arrived at 42.55 mg/g. The phosphate adsorption by the compound filler is a spontaneous endothermic process. The main mechanisms are ligand exchange and Lewis acid-base interactions; calcium and aluminum play important roles in the adsorption of phosphorus by the compound filler. Dynamic column experiments showed that as much as 90% of the phosphorus removal by compound filler, and the phosphorus concentration decreased from 1 to ~0.1mg/L. The results provide a new waste resource utilization method for PACR and show the good application potential of prepared compound filler in constructed wetlands.

Introduction

Phosphorus, as a common nutrient, is found in surface water (Boujelben et al. 2008; Xiong et al. 2017) and is related to both point and diffuse source pollution, including secondary effluent from municipal sewage treatment plants and surface runoff from agricultural activities (Cusack et al. 2019;

Mockler et al. 2017). According to statistics, 30–50% of the phosphorus in water comes from sewage treatment plant drainage (Han et al. 2019). Excessive phosphorus in watercourses leads to eutrophication and ecosystem degradation, so controlling phosphate discharge from sewage treatment plants and the continuous search for cost-effective methods for phosphorus removal have recently attracted great interest.

Numerous researchers have launched the use of constructed wetland treatment systems (CWs) as tertiary effluent filters at sewage treatment plants for phosphorus removal (Chen et al. 2016; Lu et al. 2009). The systems are designed and constructed to strengthen natural purification processes, including wetland plant uptake, substrate adsorption, chemical precipitation, and related microbial assemblage growth. Among these processes, a vital role is played by substrate adsorption and chemical precipitation in phosphorus removal (Blanco et al. 2016; Cheng et al. 2018).

Traditionally, natural materials, such as sand, gravel, unpolluted soil and gravel, are used as substrates in CWs (Brix et al. 2001; Yang et al. 2018). However, the low stability and

---

Responsible Editor: Angeles Blanco

✉ Jingqing Gao
  jingqinggao@zzu.edu.cn

✉ Zhenzhen Huang
  zzhuang@zzu.edu.cn

1 School of Ecology and Environment, Zhengzhou University, Zhengzhou 450001, China

2 School of Water Conservancy and Engineering, Zhengzhou University, Zhengzhou 450001, China

3 College of Environment, Hohai University, Nanjing 210098, China

adsorption capacity of these materials always affect the phosphorus removal efficiency (García et al. 2010). Recently, many active materials including Al, Ca, Fe, Si, and Mg have been successfully applied as substrates for phosphorus removal in CWs, such as natural materials (wollastonite (Gustafsson et al. 2008), bentonite (Chen et al. 2018), egg shells (Panagiotou et al. 2018), industrial by-products fly ash (Lu et al. 2009), steel slag (Blanco et al. 2016), water treatment sludge (Liu et al. 2016)), and man-made products lightweight aggregates (Vohla et al. 2011), cement-bound ochre pellets (Littler et al. 2013), and ceramsite (Wu et al. 2016).

In the preliminary study of our research group, non-burning substrate with cement and drinking water treatment sludge as main raw materials were prepared (Gao et al. 2020). However, more than 28% natural organic matter (NOM) is contained in drinking water treatment sludge in Zhengzhou (Henan Province, China). The release NOM is hardly biodegradable organics, and its by-products may be dangerous (Liu et al. 2016). So we are looking for a new cost-effective material that is free of NOM.

Polyaluminum chloride residue (PACR) is an inevitable by-product in the production of polyaluminum chloride. At least 60-kt PACR is produced in China every year. Although this residue is regarded a general solid waste for management purposes, its treatment has become a "burden" for production enterprises with the continuous expansion of China's coagulant industry (Han et al. 2019). For a long time, the main treatment methods of PACR were landfilling and dumping as waste. The high costs, destruction of the ecological environment, and large area required in this process pose increasingly great drawbacks. Due to the rich calcium oxide (CaO), aluminum oxide (Al_2O_3), iron oxide (Fe_2O_3), and other components in PACR, these compounds have great potential for phosphorus removal. The detailed chemical composition is shown in Supplementary Material Table A.1. Therefore, recovering useful materials from PACRs or using them to prepare other new materials will be future research trend. The direct use of raw materials in CWs will affect the normal operation of plants, microorganisms, and other wetland systems due to the weak acidity of PACR. In addition, powder adsorbents are easily lost with water flow and cause wetland clogging, restricting their extensive application in wetlands (Na et al. 2011; Yang et al. 2018). Bentonite mainly consists of the 2:1 clay mineral montmorillonite (Zhang et al. 2020). The surface roughness of bentonite improves the contact between sewage and PACR compound fillers to improve the adsorption capacity of phosphorus.

Compared with the traditional sintered filler, novel non-burning fillers have attracted much attention for their high mechanical strength, strong adsorption capacity, developed pore structure, low economic costs, low carbon emissions, environmental friendliness, and other excellent performance metrics (Gao et al. 2020). However, there have been no reports on the preparation of non-burning fillers from mainly PACR so far, and the feasibility of the production of non-burning compound fillers from PACR and its application in CWs have remained unexplored.

In this paper, a novel non-burning PACR compound filler was made from mainly PACR, Portland blast furnace slag cement, and a small amount of bentonite. The optimal proportions of addition were determined according to the results of single-factor design and mixed design tests. On this basis, the removal performance and mechanism of phosphorus were studied in detail, and the practical application value of the compound filler was evaluated.

Materials and methods

Materials

All of the chemicals used in this study were analytical grade or better. PACR was obtained from a factory in Gongyi (Zhengzhou, Henan, China). Portland blast furnace slag cement was purchased from a high-tech zone building materials market (Zhengzhou, Henan, China). Bentonite was purchased from Henan Haiyun Environmental Protection Technology Co., Ltd (Zhengzhou, Henan, China).

Preparation of compound fillers

PACR was dried at 105 °C for 4 h and passed through a 100-mesh sieve. After a large number of experiments, the final selected compound filler materials were PACR, Portland blast furnace slag cement, and bentonite. The results showed that the addition of these materials could not only neutralize the weak acidity of PACR but also significantly improve the phosphorus adsorption effect of PACR. According to the results of single-factor design and mixing design experiments (Table A.2; Figure. A.1), the optimal proportions were 44% cement, 49% PACR, and 7% bentonite. These three raw materials were evenly mixed with the indicated ratio, and the right amount of water was added (mixture/water: 3/1). After granulation by machine (XM-500, Dry powder ball press machine), the material was pressed into pellets cakes (2–4 cm) and sprinkler cured for 5–7 days until the strength was stable. The finished product is shown in Fig. 1.

Compound filler material characterization

Elemental analysis was performed by X-ray fluorescence spectrometry (XRF) using an Axios-Poly instrument. The crystal structure and phase composition of non-burning PACR compound fillers before and after phosphate adsorption were analyzed by X-ray diffraction (D8 advance diffractometer, Bruker, Germany). Fourier transform infrared

Fig. 1 Novel non-burning PACR compound filler

spectroscopy (Tensor 27, Bruker, Germany) was used to analyze the surface functional groups of the compound fillers before and after phosphate adsorption. Scanning electron microscopy–energy dispersive spectrometry (SEM-EDS) was used to analyze the surface morphology and element changes of the compound fillers before and after phosphate adsorption. The BET (Brunauer, Emmett, and Teller)-specific surface area and BJH (Barrett, Joyner, and Halenda) pore size distribution of the compound filler were determined using a specific surface area and pore analyzer (V-sorb 2800P, China) based on the nitrogen gas static adsorption method. The true density of the compound filler was measured by a true density analyzer (G-Denpyc 2900, China) based on the gas replacement method.

Static adsorption experiments

All static experiments were performed in glass conical flasks (total volume=250 mL) with 100 mL of KH_2PO_4 solution and the compound filler on a thermostatic oscillator with a speed of 150 rpm.

For kinetic studies, 1 g of compound filler was placed in KH_2PO_4 solution (total phosphorus (TP)=100 mg/L), the pH was adjusted to 7 by using HCl (0.1 M) and NaOH (0.1 M), and the mixed solution was shaken at 25 °C for different times (0.5–24 h).

For the adsorption isotherm and thermodynamic experiments, the initial TP of the KH_2PO_4 solution ranged from 50 to 300 mg/L with a compound filler dosage of 5 g/L. The mixture was shaken for 24 h at different temperatures (20, 35, and 50 °C) to reach adsorption equilibrium.

To investigate the effect of the solid concentration of the compound filler on phosphorus adsorption, different doses of compound filler (2, 4, 6, 8, 10, 12, and 14 g/L) were added to the KH_2PO_4 wastewater solution, and the mixture (pH=7) was shaken at a constant temperature (25 °C, 150 rpm) for 24 h.

Different solution pH values affect the adsorption effect of the compound filler. To study the effect of pH, 5 g/L compound filler was added to KH_2PO_4 wastewater solution (TP=100 mg/L), the solution was adjusted to different pH

values (3, 4, 5, 6, 7, 8, 9, 10, and 11) by using HCl (0.1 M) and NaOH (0.1 M), and the mixture was shaken at a constant temperature (25 °C, 150 rpm) for 24 h.

The study of coexisting anions is helpful to fully understand the potential of the best-performing fillers for further use in real CWs. Prior to the addition of compound filler, different concentrations of sodium salts (NaCl, $NaNO_3$, Na_2SO_4, and Na_2CO_3) (0–300 mg/L) were added to simulated phosphorus solution (TP=100 mg/L) to investigate the effects of coexisting anions (Cl^-, NO_3^-, SO_4^{2-}, and CO_3^{2-}). The mixture was shaken at a constant temperature (25 °C, 150 rpm) for 24 h.

To investigate the phosphorus purification effect of the compound filler on real wastewater, 1 g of compound filler was placed in domestic sewage (TP~3.4 mg/L) and with effluent of municipal sewage treatment plants (TP~1 mg/L), the mixed solution was shaken at 25 °C for different times (2–24 h).

All measurements were repeated, and the data are expressed as the mean and standard deviation of three values. After adsorption, the supernatant was centrifuged at 4000 r/min for 10 min and filtered with a 0.45-μm filter membrane. The original and residual phosphorus concentrations were determined by the potassium persulfate oxidation-molybdenum-antimony anti-spectrophotometric method. The dephosphorization rate (R%), adsorption capacity, and equilibrium adsorption capacity were calculated using the following formulas:

$$R = \frac{(C_0 - C_e)}{C_0} \times 100\% \qquad (1)$$

$$q_t = \frac{(C_0 - C_t)V}{m} \qquad (2)$$

$$q_e = \frac{(C_0 - C_e)V}{m} \qquad (3)$$

where R is the percentage of dephosphorization. q_t and q_e are the adsorption capacity and equilibrium adsorption capacity for phosphorus on the compound filler, respectively, in units of mg/g. C_0, C_t, and C_e are the concentration of

phosphorus in solution at the initial time, time t, and equilibrium, respectively, in units of mg/L. V is the volume of the solution, in units of milliliters. m is the mass of the compound filler adsorbent in units of g.

For speciation analysis of adsorbed saturated phosphorus, the adsorbed saturated compound filler was extracted successively by NH_4Cl aq, NH_4F and H_3BO_3 aq, NaOH aq, H_2SO_4 aq, $Na_3C_6H_5O_7 \cdot 2H_2O$ aq, $NaHCO_3$ aq, and $Na_2S_2O_4$ aq (Bai et al. 2017). The TP concentration of the supernatant from each round of extraction was determined after centrifugation at 4000 r/min for 10 min and filtration with a 0.45-μm filter membrane.

For regeneration of adsorbed saturated compound filler, 1g adsorbed saturated compound filler was placed in an Erlenmeyer flask containing 0.1 mol/L hydrochloric acid solution, sodium hydroxide solution, and sodium chloride solution (50 mL). After shaking at 25 °C for 2 h, the compound filler was washed with distilled water, and then taken out after drying. The phosphorus removal of the regenerated compound filler in 100 mg/L phosphorus solution was measured, and so on.

Dynamic column adsorption experiments

To assess the phosphate removal effect of compound filler under dynamic flow condition, two experimental devices of dynamic adsorption column with an inner diameter of 10 cm and a height of 40 cm were established (Figure A.5). The influent solution was collected from the secondary effluent of municipal sewage treatment plants with TP concentration of ~1mg/L and pumped into the column in an up-flow mode. The compound filler was filled with 1.5 kg (height 90 cm) and effective volume was 1150 mL, respectively. The flow rate of peristaltic pump was 0.799 mL/min. The column hydraulic time (HRT) was 24 h. The phosphorus concentration and pH of influent and effluent were measured daily.

Results and discussion

Properties of the compound filler

The prepared compound filler based on the best formula was determined by single-factor design and mixing design taking phosphorus adsorption and strength into account. The compound filler was placed in 25 °C conditions for 6 h, the surface was allowed to dry, and the strength was stable after 7 days of sprinkler curing. As a wetland filler, the material needs to have enough strength and a good pore size to take advantage of its excellent phosphorus adsorption ability. Specific compound filler physical performance parameters are presented in Table 1. The principal chemical composition of the compound filler measured by XRF is shown in Table A.3. It can be seen

Table 1 Physical performance parameters of compound filler

Filler parameter	Numerical value
Compressive strength	480 N
True density	2.455 g/mL
Multipoint-specific surface area	29.290 m^2/g
Packing density	820 kg/m^3
Median pore diameter	0.546 nm
Micropore surface area	28.971 m^2/g

from Table A.3 that the main chemical components of the compound filler were silicon, calcium, aluminum, iron, and a small amount of other elements, and does not contain heavy metal ions.

Static adsorption characteristics of phosphorus

Adsorption kinetics

The kinetics of phosphate adsorption by the compound filler are presented in Fig. 2. It is concluded that the process of phosphate adsorption by the compound filler involved rapid adsorption and slow equilibrium. A similar adsorption trend was also found in the removal of phosphate by sewage sludge adsorbents and alum sludge (Jiang et al. 2017; Yang et al. 2006). The equilibrium adsorption capacity reached 15.32 mg/g, and the phosphorus removal rate exceeded 99%.

Four kinetic equations (Eqs. (4)–(7)) were used to correlate the phosphorus sorption data to understand phosphate sorption processes on the compound filler; the equations are as follows (Chen et al. 2018):

$$Pseudo-first-order\,equation\,(PFO):\ln(q_e-q_t)$$

$$=\ln q_e - k_1 t \tag{4}$$

$$Pseudo-second-order\,equation\,(PSO):\frac{t}{q_t}=\frac{1}{k_2}q_e^2+\frac{t}{q_e} \tag{5}$$

$$Simple\,Elovich\,equation\,(SE):q_t=a+b\,lnt \tag{6}$$

$$Intra-particle\,diffusion\,equation\,(IPD):q_t=k_p t^{\frac{1}{2}}+c \tag{7}$$

where q_e and q_t (mg/g) are the adsorption capacities of phosphorus at equilibrium and at any time t (h), respectively. k_1 (1/h) is the rate constant of the PFO equation; k_2 (g/mg×h) is the rate constant of the PSO equation; a (mg/g) and b (mg/g×h) are the desorption constants of the SE equation, respectively; and k_p (mg/g×h$^{1/2}$) and c (mg/g) are the rate constants of the IPD model, respectively.

The resulting parameters of the four kinetic fitting equations are shown in Table A.4. The pseudo-second-order model
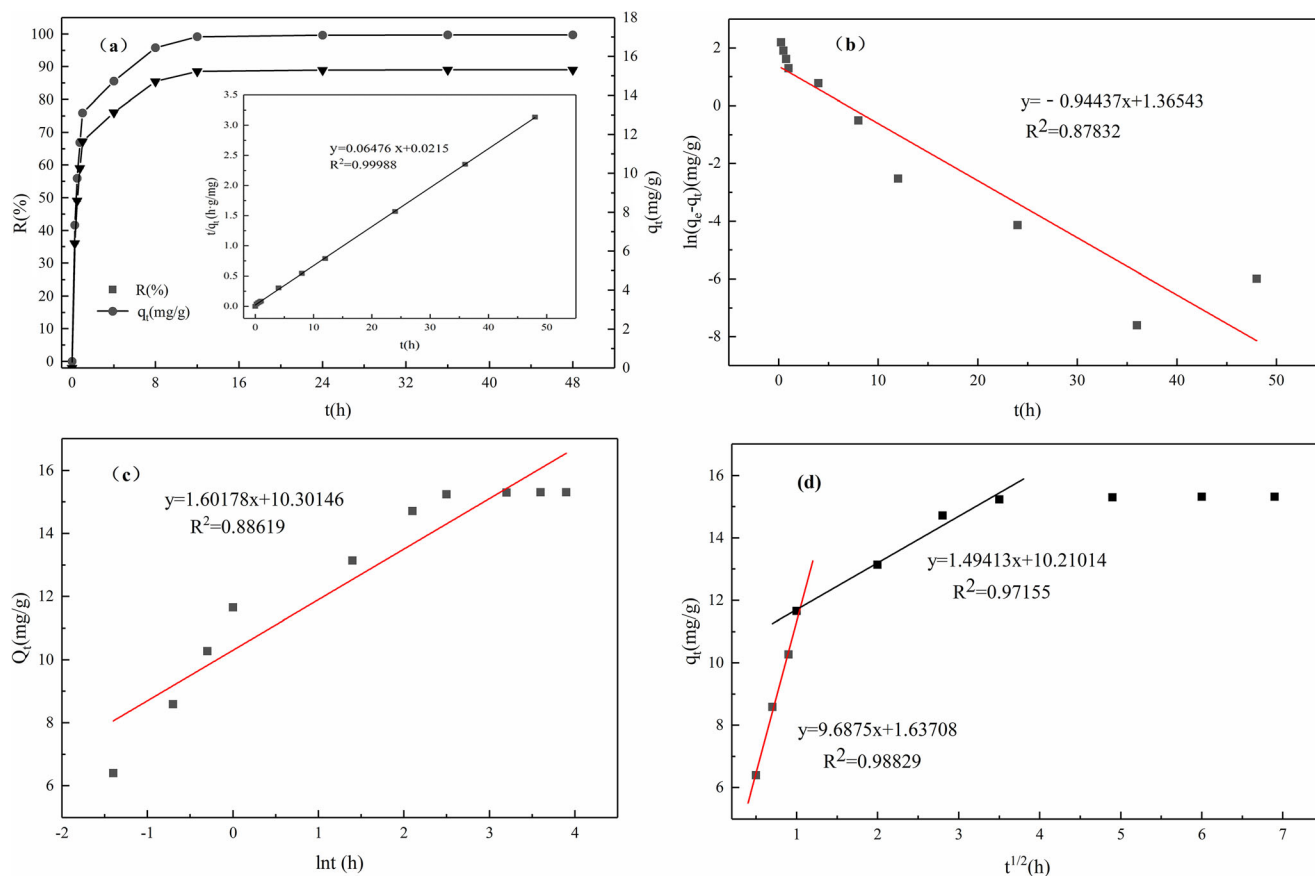
Fig. 2 Adsorption kinetic curves of phosphorus onto compound filler and pseudo-second-order equation (**a**), pseudo-first-order equation (**b**), Elovich equation (**c**), and intra-particle diffusion equation (d)

can better describe the adsorption kinetic results (R^2=0.99988) than the pseudo-first-order model (R^2=0.87832) and the Elovich equation (R^2=0.88619), indicating that the rate-controlling mechanism was involved chemical interaction (Kuśmierek et al. 2016; Liu et al. 2015). The calculated q_e was 15.44 mg/g, which is close to the experimental value (15.32 mg/g).

For compound fillers, there are several stages associated with transport processes during adsorption: bulk transport, film diffusion, intra-particle diffusion, and adsorptive attachment (Hai et al. 2017; Weber and Smith 1987). As seen from the intra-particle diffusion model, the adsorption process includes two stages. The first linear region describes film diffusion, and the second linear region describes intra-particle diffusion. The linear portions of the curves do not pass through the origin, indicating that the mechanism of phosphate adsorption is complex and that both surface adsorption and intra-particle diffusion are involved in the actual adsorption process (Özer et al. 2005). In addition, comparing the two diffusion constants of K_{p1} and K_{p2}, as shown in Table A.4, reveals that K_{p1} is approximately six times higher than K_{p2}, which suggests that intra-particle diffusion may be the decisive step of the adsorption process (Özer et al. 2005; Zhang and Leiviskä 2020).

Adsorption isotherm

As seen from the Fig. A.2, increasing the initial phosphorus concentration and temperature significantly increased the phosphorus adsorption capacity of the compound filler. This is because the migration rate of phosphorus on the compound filler accelerated as the temperature increased, speeding up the mass transfer between the phosphorus and the compound filler (Lan et al. 2018).

The Langmuir and Freundlich models are usually used to further analyze the type of adsorption (Chung et al. 2015). The Langmuir adsorption isotherm is a theoretical formula, which holds that the adsorbents form a single-molecule adsorption layer on the surface of a uniform solid and there is no intermolecular force (Baseri and Tizro 2017). The Freundlich adsorption isotherm is an empirical formula that describes multilayer adsorption and heterogeneous surface adsorption (Coles and Yong 2006). As expressed (Fu et al. 2011):

$$\frac{C_e}{q_e} = \frac{1}{K_L q_m} + \frac{1}{q_m} c_e \tag{8}$$

$$ln q_e = ln K_F + \frac{1}{n} ln C_e \tag{9}$$

where q_e (mg/g) and C_e (mg/L) are the adsorption amount and concentration of phosphorus at equilibrium, respectively. q_m (mg/g) represents the maximum adsorption capacity of the Langmuir model, and K_L (L/mg) is the Langmuir constant related to the adsorption energy. K_F (L/mg) is the Freundlich constant related to adsorption capacity, and n is the heterogeneity factor indicating the adsorption strength of the adsorbate, where the larger the n value is, the stronger the adsorption force.

The values of the Langmuir and Freundlich constants and of the correlation coefficients for the compound filler are presented in Table 2. The results showed that the isotherm data could be fitted by both the Langmuir and Freundlich models, and the Freundlich isotherm model was slightly better fit to the experimental data than the Langmuir model, which indicated that the compound filler provides both a homogeneous monolayer and heterogeneous active sites for phosphorus adsorption (Yang et al. 2006; Yin et al. 2016). Moreover, adsorption by heterogeneous active sites was slightly stronger than that by other sites on the compound filler.

As shown in Table 3, the maximum phosphate adsorption capacity of the compound filler determined from the Langmuir isotherm plot was 42.55 mg/g, which is 260–21,150 times that of sand (Arias et al. 2001), 12–61 times that of dewatered alum sludge (Yang et al. 2006), 10 times that of natural materials such as turf (Cui et al. 2008), 6 times that of man-made biochar (Jung et al. 2015), 9–12 times that of CFA/WS/OS ceramsite (Cheng et al. 2018), 179 and 6 times that of natural and thermally treated bentonite (Chen et al. 2018), respectively, 16–76 times that of fly ash pellets, and 19 times that of steel slag (Drizo et al. 2006).

Adsorption thermodynamics

Adsorption thermodynamics are mainly concerned with the degree to which adsorption can be achieved. By studying the adsorption amount of adsorbates on adsorbents under various conditions, various thermodynamic data can be obtained, such as the diffusion coefficient (K_d), Gibbs free energy ($\Delta G°$), enthalpy change ($\Delta H°$), and entropy change ($\Delta S°$) (Ma et al. 2020). The standard Gibbs free energy change is calculated according to the following formulas:

Table 2 Parameters of Langmuir and Freundlich isotherm for phosphate adsorption onto compound filler

Temperature (°C)	Langmuir equation			Freundlich equation		
	Q_m	K_L	R^2	n	K_F	R^2
20	42.55	0.443	0.98249	3.207	9.833	0.99343
35	40.05	0.395	0.98283	3.272	10.998	0.99967
50	39.62	0.306	0.97554	3.574	13.013	0.99790

Table 3 Comparison of adsorption capacities of phosphate with different types of substrates in CWs

Type of substrate in CWs	P adsorption (mg/g)	References
Sand	0.02–0.17	(Arias et al. 2001)
Dewatered alum sludge	0.7–3.5	(Yang et al. 2006)
Turf	4.24	(Cui et al. 2008)
Man-made biochar	6.79	(Jung et al. 2015)
CFA/WS/OS ceramsite	3.48–4.51	(Cheng et al. 2018)
Natural bentonite	0.24	(Chen et al. 2018)
Thermally treated bentonite	6.94	(Chen et al. 2018)
Fly ash pellets	0.59–2.56	(Drizo et al. 2006)
Steel slag	2.2	(Drizo et al. 2006)
Compound filler	42.55	This study

$$K_d = \frac{C_0 - C_e}{C_e} \times \frac{V}{m} \tag{10}$$

$$lnK_d = -\frac{\Delta H°}{RT} + \frac{\Delta S°}{R} \tag{11}$$

$$\Delta G° = \Delta H° - T\Delta S° \tag{12}$$

where C_0 is the initial adsorption concentration, C_e is the adsorption equilibrium concentration (mg/L), K_d is the solid-liquid distribution coefficient (mL/g), m is the mass of adsorbent, V is the volume of the solution (mL), T is the temperature (K), and R is the gas constant (J/mol•K).

As seen from Table A.5, K_d value increases with increasing temperature, and $\Delta H > 0$ and $\Delta G < 0$ in the phosphate adsorption process, which indicates that the adsorption of phosphate by the compound filler is a spontaneous endothermic process (Raganati et al. 2018). The free energy ΔG is the embodiment of the adsorption driving force. With increasing temperature, the absolute value of ΔG increases, indicating that a greater driving force is obtained in the adsorption process and that an increase in temperature promotes adsorption (Tran et al. 2018). In addition, the variations in ΔG at different initial concentrations show that phosphate adsorption by compound filler is not a single physical or chemical adsorption process, but the coexistence of physical adsorption and chemical adsorption processes. Phosphate adsorption is accompanied by the desorption of other ions, i.e., via ion exchange or ligand exchange.

The effects of operational parameters

Regarding the effect of compound filler dosage on adsorption, Fig. 3 a shows that the removal rate of phosphorus increased significantly from 51 to 99% with an increase of compound
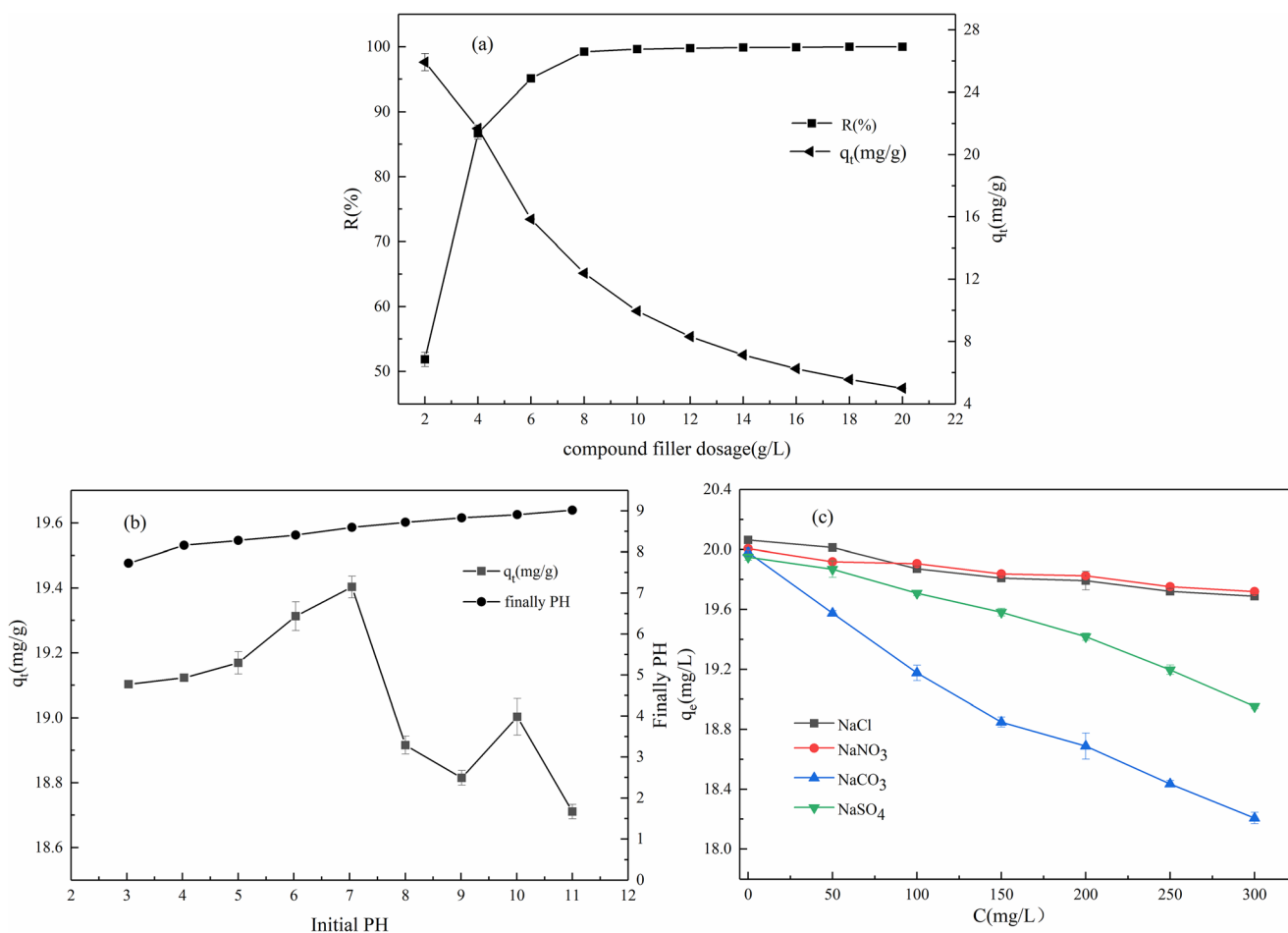
Fig. 3 The effect of compound filler dosage (**a**); the effect of initial pH value on phosphate adsorption capacity and finally pH after adsorption of compound filler (**b**); the effect of Cl$^-$, NO$_3^-$, SO$_4^{2-}$, CO$_3^{2-}$ on equilibrium adsorption capacity of compound filler (**c**)

filler dosage from 2 to 10 g/L. However, when the compound filler adsorbent dosage was further increased, the removal rate of phosphorus increased negligibly. On the other hand, the phosphorus adsorption capacity gradually decreased from 26 to 7 mg/g with increasing compound filler dosage. Given the economy (minimum compound filler usage) and efficiency (phosphorus removal rate above 99.5%) of such operation, the optimal concentration of compound filler was 10 g/L, at which value both the adsorption capacity and percentage were maintained at high levels.

The initial solution pH value can significantly affect the phosphate adsorption capacity of a compound filler during the adsorption process (Wei et al. 2008; Xiong et al. 2019). An increase in pH value from 3 to 11 influenced phosphate adsorption, mainly due to the dissolution of cations, the total surface charge of the adsorbent, and the species of phosphate in solution (Chouyyok et al. 2010; Gan et al. 2009). As the pH increased from 2 to 12, the forms of phosphate changed from H$_2$PO$_4^-$ to HPO$_4^{2-}$ and PO$_4^{3-}$ (Chouyyok et al. 2010; Yang et al. 2013). As the pH value increased from 4 to 9, HPO$_4^{2-}$

became the dominant species, which was not conducive to ligand exchange since the free energy of adsorption of HPO$_4^{2-}$ is higher than that of other species, and the adsorption capacity of the adsorbent decreased accordingly (Lin et al. 2017). In addition, a high pH value could cause the compound filler surface to carry more OH$^-$, which may cause competition for adsorption sites on the compound filler among HPO$_4^{2-}$, PO$_4^{3-}$ and OH$^-$ in solution (Babatunde et al. 2009; Su et al. 2013). Figure 3 b shows that the compound filler could act as a buffer solution to neutralize alkaline and acidic conditions. When the initial pH was acidic or neutral, the distinct change in solution pH indicated that surface hydroxide groups and phosphate underwent ligand exchange (Liu et al. 2011; Zhang et al. 2011). As the initial pH increased, the value of the solution pH decreased. This is because of the deprotonation of coordination water molecules at the metal active sites (Wu et al. 2007). This phenomenon revealed that a ligand exchange mechanism may not occur within this pH range and that phosphate removal might occur through a Lewis acid-base interaction mechanism (Liu et al. 2013). In summary, ligand

exchange and Lewis acid-base interactions took place in the phosphate adsorption process, and the adsorption mechanisms were highly dependent on the pH value of the initial solution (Blaney et al. 2007; Collins et al. 1999; Yang et al. 2013).

The coexisting anions investigated were Cl^-, NO_3^-, SO_4^{2-}, and CO_3^{2-}. The results are shown in Fig. 3 c. The presence of Cl^-, NO_3^-, SO_4^{2-}, and CO_3^{2-} inhibited phosphate sorption by the compound filler to varying degrees. Of all the coexisting anions investigated, with increases in the coexisting anion concentration, SO_4^{2-} and CO_3^{2-} had a slightly greater effect on phosphorus removal, whereas the effects of Cl^- and NO_3^- on phosphorus removal were limited. This may be related to the geometry of anions, which have various shapes, including spherical (Cl^-), linear (OH^-), triangular (NO_3^-, CO_3^{2-}), and tetrahedral (PO_4^{3-}, SO_4^{2-}) (Wu et al. 2019). In general, an inner-sphere complexation through the ligand exchange process may consist of a phosphate molecule connected by one or two metal atoms to one or two oxygen bonds, other anions such as Cl^-, NO_3^-, and CO_3^{2-} generally form an outer-sphere complexation (a water molecule exists between the ions and the surface of metal oxide), while sulfate can form an inner and outer spherical complexation on the surface of metal oxides (Wu et al. 2019; Liu et al. 2018). Compared with outer-sphere complexation, inner-sphere complexation has stronger interactions, thus phosphate can be selectively sorbed by the compound filler compared to other anions. Besides, these results can be explained by Hard and soft Acids and Bases (HSAB) theory (Pearson 1968). This concept describes a species' preference for other species of the same compound when forming coordinative bonds: hard acids prefer to coordinate with hard bases, while soft acids prefer to coordinate with soft bases (Beer and Gale 2001; Pearson 1968). The results show that phosphate is a hard base, and hard acid metals such as Fe^{3+}, Al^{3+}, Mg^{2+}, and Ca^{2+} have good phosphate complexation properties. In addition, other anions, such as OH^-, Cl^-, NO_3^-, SO_4^{2-}, and CO_3^{2-}, also belong to the hard bases. However, the electron pair-donating capacity (or Lewis basicity) of these anions is different and follows the order of $PO_4^{3-} > CO_3^{2-} > SO_4^{2-} > Cl^- > NO_3^-$. This trend may indicate a difference in the complexation ability of these anions with a given Lewis acid metal. The HSAB theory can offer a preliminary explanation for why the compound filler has high selectivity for phosphate even if coexisting anions are present at several times the phosphate concentration.

To understand the purification effect of compound filler on actual wastewater is helpful to evaluate the phosphorus removal performance of compound filler. The results are shown in Fig. A. 4, The phosphorus removal rate of the compound filler in the domestic sewage (TP~3.4 mg/L) and effluent of municipal sewage treatment plants (TP~1 mg/L) can reach more than 99% in 2h, and have good phosphorus retention ability, without obvious desorption phenomenon.

Characterization of compound fillers before and after adsorption

The surface functional groups of the compound filler before and after adsorption were determined by FTIR spectroscopy. The results are shown in Fig. 4 a; the FTIR spectra exhibited several functional groups. For example, the absorption peaks at 3431 cm^{-1} before adsorption and 3441 cm^{-1} after adsorption were assigned to –OH bending vibrations and were strengthened after the adsorption of phosphate (Jiang et al. 2017), which indicated that metal ions could also be hydroxylated in the solution. In addition, the peak at 1038 cm^{-1} was significantly enhanced after adsorption compared to that before adsorption, and the appearance of a new peak at 561 cm^{-1}, which was intense and broad, could be assigned to the asymmetric vibration of P–O bonds (Berzinacimdina and Borodajenko 2012), indicating that an interaction might exist between surface hydroxyl groups and phosphate (Su et al. 2013; Wang et al. 2018).
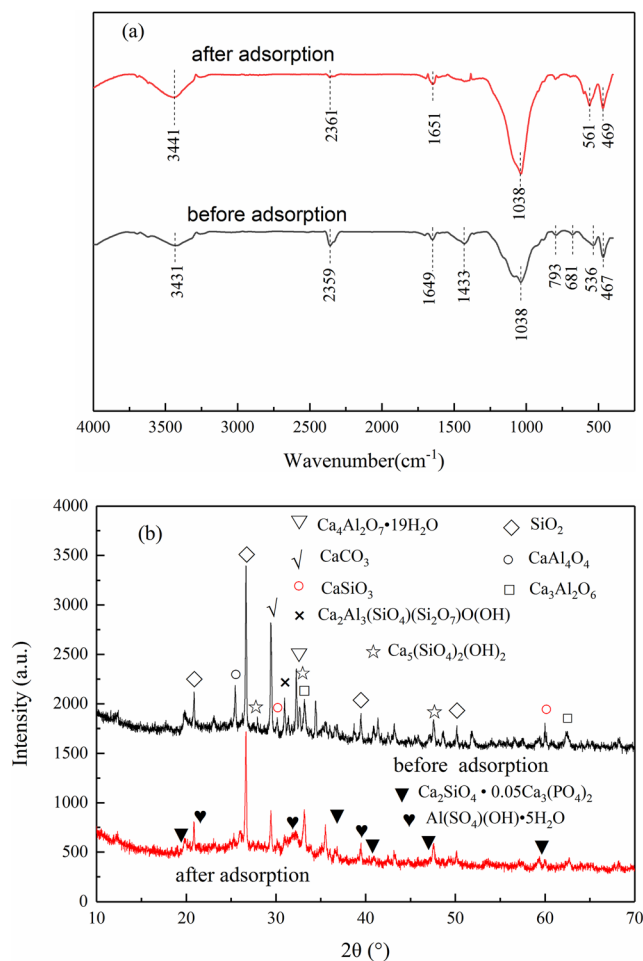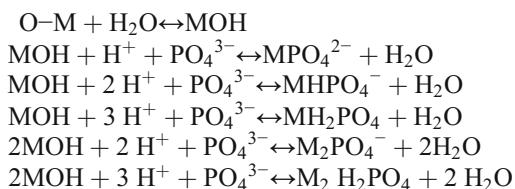

Fig. 4 FTIR spectra of compound filler before and after phosphate adsorption (**a**) and X-ray diffraction of compound filler before and after phosphate adsorption (**b**)

Figure 4 b shows X-ray diffraction patterns of the compound filler before and after the phosphate reaction. Jade 6.5 was used to analyze the characteristic diffraction peaks at different 2θ (°), and the results showed that the main components of the compound filler were quartz, calcite, calcium silicate, calcium aluminum oxide, and reinhardbraunsite. These chemicals have great potential for phosphorus removal and have been reported in other relevant research (Cheng et al. 2018; Lu et al. 2009; Oguz 2005; Yu et al. 2010). After the phosphate adsorption process, the crystallization peaks related to elements such as calcium and aluminum were weakened to a certain extent, which indirectly proved that elements such as calcium and aluminum played an important role in the process of phosphorus removal. In combination with the appearance of calcium phosphate silicate, we infer that the dominant mechanism for the adsorption of phosphate by compound fillers is inner-sphere complexation via the ligand exchange process (Li et al. 2016; Ruiting et al. 2018). In reaction solution, the surface of metal oxides is usually covered by hydroxyl groups. During the ligand exchange process, these surface hydroxyl groups are replaced by other ligands, such as phosphate, which form covalent chemical bonds with metal atoms. The interactions between the compound filler and phosphate can be described as follows:

$$O{-}M + H_2O \leftrightarrow MOH$$
$$MOH + H^+ + PO_4{}^{3-} \leftrightarrow MPO_4{}^{2-} + H_2O$$
$$MOH + 2\,H^+ + PO_4{}^{3-} \leftrightarrow MHPO_4{}^- + H_2O$$
$$MOH + 3\,H^+ + PO_4{}^{3-} \leftrightarrow MH_2PO_4 + H_2O$$
$$2MOH + 2\,H^+ + PO_4{}^{3-} \leftrightarrow M_2PO_4{}^- + 2H_2O$$
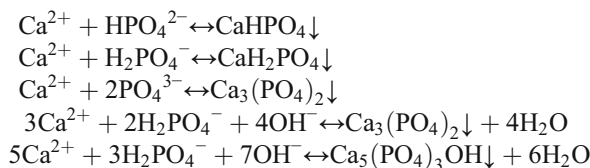$$2MOH + 3\,H^+ + PO_4{}^{3-} \leftrightarrow M_2\,H_2PO_4 + 2\,H_2O$$

where M and OH represent the metal atom and the hydroxyl group, respectively (Xie et al. 2014). Figure 5 summarizes the possible mechanisms for phosphorus sorption by compound filler.
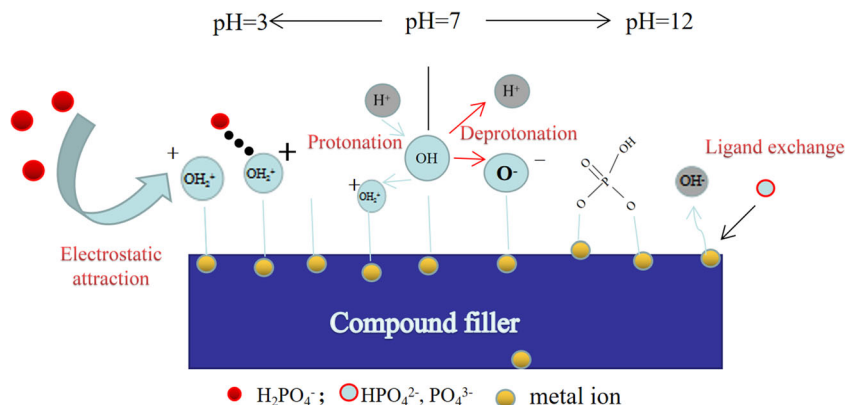
A layer of white precipitate was deposited in the glass container after the adsorption reaction and could be dissolved with dilute hydrochloric acid. It was speculated that the dissolved metal ions in the compound filler react with phosphate. The involved reactions are as follows (Jie et al. 2013):

$$Ca^{2+} + HPO_4{}^{2-} \leftrightarrow CaHPO_4\downarrow$$
$$Ca^{2+} + H_2PO_4{}^- \leftrightarrow CaH_2PO_4\downarrow$$
$$Ca^{2+} + 2PO_4{}^{3-} \leftrightarrow Ca_3(PO_4)_2\downarrow$$
$$3Ca^{2+} + 2H_2PO_4{}^- + 4OH^- \leftrightarrow Ca_3(PO_4)_2\downarrow + 4H_2O$$
$$5Ca^{2+} + 3H_2PO_4{}^- + 7OH^- \leftrightarrow Ca_5(PO_4)_3OH\downarrow + 6H_2O$$

As shown in Fig. 4 b, there was no significant change in the peak of quartz before and after reaction. Therefore, quartz plays a minor role in the phosphorus removal process. To test this hypothesis, a separate experiment of phosphorus removal by quartz sand was designed. Unfortunately, the average concentration of phosphorus in the solution decreased from 108.1 to 108 mg/L after 24 h, the removal rate was only 0.09%, and the removal effect was negligible. A similar conclusion has also been reported in the literature (Delaney et al. 2011).

To better understand the surface morphology and element changes before and after phosphate adsorption by the compound filler, SEM-EDS analysis was conducted. Figure 6 a shows that the compound filler surface was rough, cracked, and loose and that a large number of pores were distributed on the surface. The rough surface is beneficial to improving contact between the compound filler and the adsorbent, and the numerous pores expand the specific surface area of the compound filler to facilitate adsorption at surface active sites. Figure 6 b reveals that the surface of the compound filler was obviously covered with a layer of crystalline material and relatively smooth with few pores after the adsorption of phosphate, which further proved that ligand exchange occurred mainly at the compound filler surface active sites (Gao et al. 2020; Yang et al. 2015). As seen from Fig. 6 c and d, the changes in the main elements on the surface of the compound filler before and after adsorption indicated that

Fig. 5 Schematic diagram of the possible mechanisms for phosphorus adsorption by compound filler

Fig. 6 SEM observations of compound filler before (**a**) and after (**b**) phosphate adsorption; EDS spectrum of compound filler before (**c**) and after (**d**) phosphate adsorption
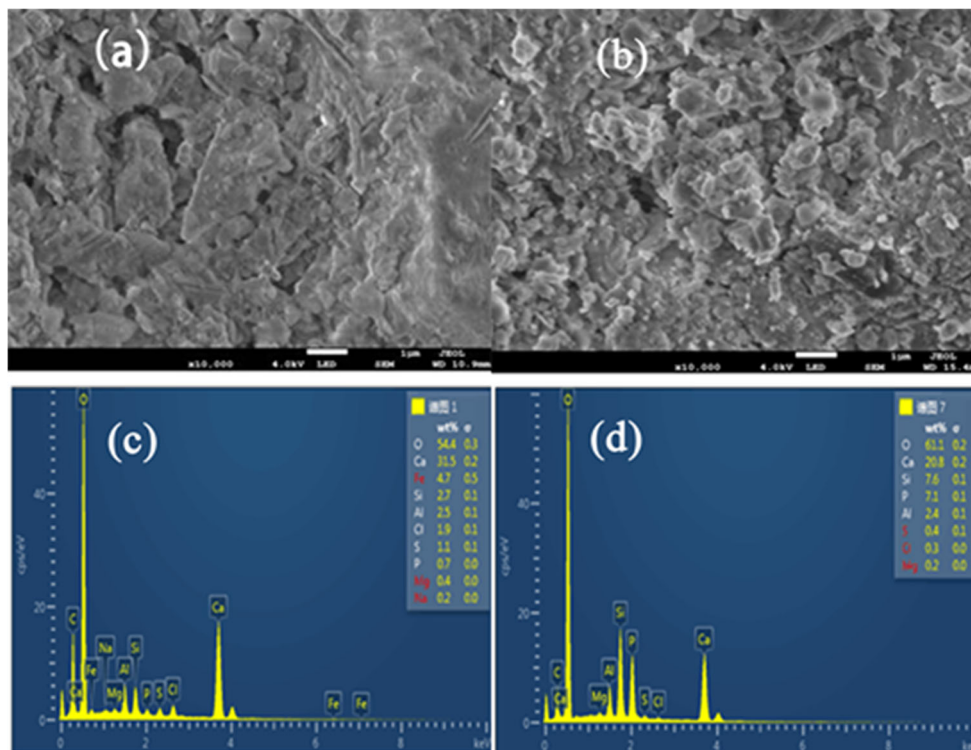
calcium, aluminum, and iron played greater roles than other elements in the adsorption process, and the peaks of phosphorus and oxygen were significantly enhanced after adsorption.

Speciation analysis of saturated adsorbed phosphorus

To further study the mechanism of phosphorus removal by adsorption by the compound filler, the sequential graded extraction method was used to distinguish the adsorbed phosphorus into soluble adsorbed phosphorus (S–P, extracted by NH_4Cl aq.), aluminum adsorbed phosphorus (Al–P, extracted by NH_4F, H_3BO_3 aq.), iron adsorbed phosphorus (Fe–P, extracted by NaOH aq.), calcium adsorbed phosphorus (Ca–P, extracted by H_2SO_4 aq.), and occluded phosphorus (O–P, extracted by $Na_3C_6H_5O_7 \cdot 2H_2O$, $NaHCO_3$, and $Na_2S_2O_4$ aq.). Figure 7 indicates that Ca–P and Al–P were the dominant adsorption forms, accounting for 59% and 23%, respectively. In addition, approximately 2.39% of the adsorption amount of phosphate was Fe–P, and the soluble phosphorus and occluded phosphorus contents were also low. This result was also consistent with the SEM-EDS results.

Regeneration of adsorbed saturated compound filler

Adsorbents recycling is an important factor affecting the application prospect of adsorbents. As shown in Fig. A.3, NaCl solution was not suitable for exchanging phosphate from compound filler when compared with the other two desorption

solution. These results were due to the low affinity of Cl^- with compound filler (Cheng et al. 2009). However, with the increase of the number of regenerations, the phosphorus removal rate of the compound filler decreases significantly. After being regenerated by HCl and NaOH solutions for the fourth time, the phosphate removal rate of the compound filler were only 70% or 55%, respectively. On the one hand, hydrogen ions make desorption of the saturated compound filler more complete, releasing more active sites, but at the same time causing the loss of some metal ions (Wu et al. 2019). On the
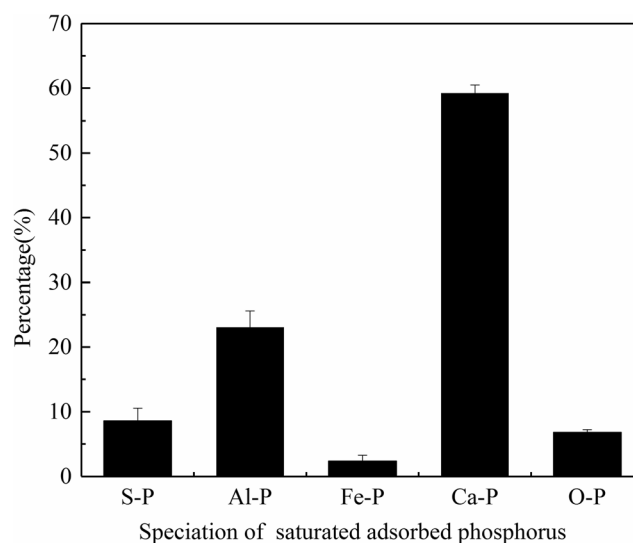

Fig. 7 Speciation analysis of saturated adsorbed phosphorus onto compound filler

other hand, the hydroxide group and the bound phosphate on the surface of the compound filler compete for adsorption sites to promote the release of phosphorus, but caused certain damage to the compound filler (Gao et al. 2020). This limits the number of regeneration of adsorbed saturated compound filler.

Dynamic column adsorption experiments

Figure 8 presents effluent pH of compound filler packed column. The influent sewage pH was about 6.5, but the initial effluent was somewhat alkaline, which may be caused by the hydrolysis of metal ions on the compound filler. In addition, during the adsorption process, the pH of the effluent is slightly higher than the influent. This result was also consistent with previous static test results.

Figure 8 shows the effect of HRT 24 h on the removal of phosphorus by compound filler packed column. The phosphorus removal rate of the compound filler packed column reached up to 90% with a stable effluent concentration of phosphorus (~0.1 mg/L), which basically reached the surface water quality of ClassII (GB 3838-2002) (Environmental Protection Agency of China 2002). These indicates that the compound filler has the higher potential to effectively remove the phosphorus as the CWs substrate under the condition of dynamic flow condition.

Application potential of compound filler in CWs

Suppose compound filler is used in CWs, take the CWs with a daily treatment capacity of 10,000 t/day sewage as an example, an effective CWs area of 40,000m^2 (60 mu), and a depth of 0.7m, only half of the CWs substrate contains compound filler, the compound filler was used for 11,200m^3 (according to the project
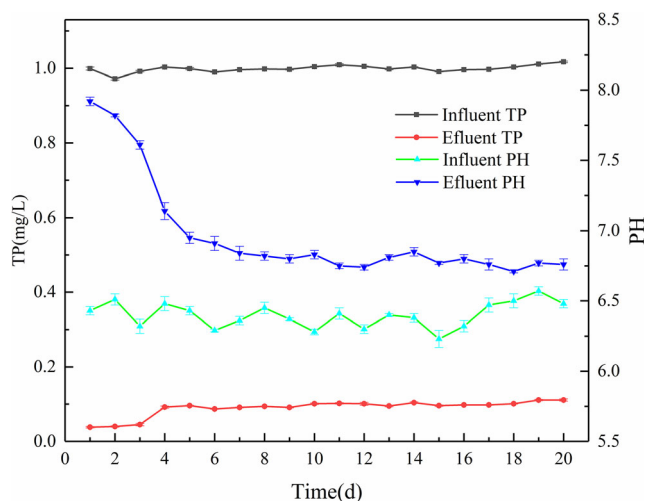

Fig. 8 Dynamic adsorption of phosphorus by compound filler packed column: change of influent and effluent TP; change of influent and effluent ph

experience value). Based on the phosphorus adsorption capacity of compound filler (15 mg/g), the adsorption life of the compound filler to phosphorus is up to 46 years theoretically. In addition, research shows the *P. aeruginosa* can promote the release of Ortho-P from adsorbents into the liquid phase, which may promote plant growth (Wang et al. 2020). Moreover, because the Ca–P is more easily absorbed by plants than Al–P and Fe–P (Mitrogiannis et al. 2017), the adsorbed phosphorus of compound filler are more conductive to the growth of constructed wetlands plants (the adsorbed phosphorus form is mainly Ca–P), which further improves the phosphorus adsorption life of the compound filler in CWs. Therefore, the application of compound filler in CWs is very sensible and practical, and it has a good synergistic effect with microorganism and plant in CWs. Taken together, the actual adsorption life of the compound filler needs further observation in the CWs project.

Considering various factors, the cost of the compound filler is 180 yuan/t, which is far lower than 250 yuan/t for gravel and 450 yuan/t for ceramsite in China. The low cost, high adsorption performance, and long adsorption life make it have good application potential in CWs.

Conclusions

In our study, an efficient and non-burning PACR compound filler has been successfully prepared for the first time by using PACR as the main materials, which provides a new method for the reuse of PACR waste resources. The phosphorus adsorption performance and mechanisms of the compound filler were explored completely. The PACR compound filler possessed high selectivity to phosphorus adsorption, almost without influence of other factors, and exhibited excellent phosphorus adsorption efficiency (99.9%) and adsorption capacity (42.55 mg/g). Moreover, the phosphorus adsorption of compound filler is the coexistence of physical adsorption and chemical adsorption process. The main mechanism is ligand exchange and Lewis acid-base interactions, calcium and aluminum play important roles in the phosphorus adsorption. In addition, column experiments indicated the compound filler could effectively remove phosphorus under dynamic flow conditions. Meanwhile, microorganisms and plants have a good synergistic effect on the phosphorus adsorption life of compound filler. The results obtained are of great significance in resource utilization of PACR and application of fillers in CWs.

Declarations

Ethics approval   Not applicable.

Consent to participate   Not applicable.

Consent to publish   Not applicable.

Competing interests   The authors declare no competing interests.

References

Arias CA, Bubba MD, Brix H (2001) Phosphorus removal by sands for use as media in subsurface flow constructed reed beds. Water Res 35(5):1159–1168. https://doi.org/10.1016/S0043-1354(00)00368-7

Babatunde AO, Zhao YQ, Burke AM, Morris MA, Hanrahan JP (2009) Characterization of aluminium-based water treatment residual for potential phosphorus removal in engineered wetlands. Environ Pollut 157(10):2830–2836. https://doi.org/10.1016/j.envpol.2009.04.016

Bai J, Ye X, Jia J, Zhang G, Zhao Q, Cui B, Liu X (2017) Phosphorus sorption-desorption and effects of temperature, pH and salinity on phosphorus sorption in marsh soils from coastal wetlands with different flooding conditions. Chemosphere 188:677–688. https://doi.org/10.1016/j.chemosphere.2017.08.117

Baseri H, Tizro S (2017) Treatment of nickel ions from contaminated water by magnetite based nanocomposite adsorbents: effects of thermodynamic and kinetic parameters and modeling with Langmuir and Freundlich isotherms. Process Saf Environ Prot 109:465–477. https://doi.org/10.1016/j.psep.2017.04.022

Beer PD, Gale PA (2001) Anion recognition and sensing: the state of the art and future perspectives. Angew Chem Int Ed 40(3):486–516. https://doi.org/10.1002/1521-3773(20010202)40:33.0.CO;2-P

Berzina-Cimdina L, Borodajenko N (2012) Research of calcium phosphates using Fourier transform infrared spectroscopy, SourceInTech. Infrared Spectroscopy—Materials Science, Engineering and Technology. Edited by Prof. Theophanides Theophile pp 123–148. https://doi.org/10.5772/36942

Blanco I, Molle P, Saenz de Miera LE, Ansola G (2016) Basic oxygen furnace steel slag aggregates for phosphorus treatment. Evaluation

of its potential use as a substrate in constructed wetlands. Water Res 89:355–365. https://doi.org/10.1016/j.watres.2015.11.064

Blaney LM, Cinar S, Sengupta AK (2007) Hybrid anion exchanger for trace phosphate removal from water and wastewater. Water Res 41(7):1603–1613. https://doi.org/10.1016/j.watres.2007.01.008

Boujelben N, Bouzid J, Elouear Z, Feki M, Jamoussi F, Montiel A (2008) Phosphorus removal from aqueous solution using iron coated natural and engineered sorbents. J Hazard Mater 151(1):103–110. https://doi.org/10.1016/j.jhazmat.2007.05.057

Brix H, Arias CA, Bubba Md (2001) Media selection for sustainable phosphorus removal in subsurface flow constructed wetlands. Water Sci Technol 44(1112):47–54. https://doi.org/10.2166/wst.2001.0808

Chen Z, Cuervo DP, Müller JA, Wiessner A, Koser H, Vymazal J, Kastner M, Kuschk P (2016) Hydroponic root mats for wastewater treatment—a review. Environ Sci Pollut Res 23(16):15911–15928. https://doi.org/10.1007/s11356-016-6801-3

Chen X, Wu L, Liu F, Luo P, Zhuang X, Wu J, Zhu Z, Xu S, Xie G (2018) Performance and mechanisms of thermally treated bentonite for enhanced phosphate removal from wastewater. Environ Sci Pollut Res 25(16):15980–15989. https://doi.org/10.1007/s11356-018-1794-8

Cheng X, Huang X, Wang X, Zhao B, Chen A, Sun D (2009) Phosphate adsorption from sewage sludge filtrate using zinc-aluminum layered double hydroxides. J Hazard Mater 169(1-3):958–964. https://doi.org/10.1016/j.jhazmat.2009.04.052

Cheng G, Li Q, Su Z, Sheng S, Fu J (2018) Preparation, optimization, and application of sustainable ceramsite substrate from coal fly ash/waterworks sludge/oyster shell for phosphorus immobilization in constructed wetlands. J Clean Prod 175:572–581. https://doi.org/10.1016/j.jclepro.2017.12.102

Chouyyok W, Wiacek RJ, Pattamakomsan K, Sangvanich T, Grudzien RM, Fryxell GE, Yantasee W (2010) Phosphate removal by anion binding on functionalized nanoporous sorbents. Environ Sci Technol 44(8):3073–3078. https://doi.org/10.1021/es100787m

Chung HK, Kim WH, Park J, Cho J, Jeong TY, Park PK (2015) Application of Langmuir and Freundlich isotherms to predict adsorbate removal efficiency or required amount of adsorbent. J Ind Eng Chem 28:241–246. https://doi.org/10.1016/j.jiec.2015.02.021

Coles CA, Yong RN (2006) Use of equilibrium and initial metal concentrations in determining Freundlich isotherms for soils and sediments. Eng Geol 85(1):19–25. https://doi.org/10.1016/j.enggeo.2005.09.023

Collins CR, Ragnarsdottir KV, Sherman DM (1999) Effect of inorganic and organic ligands on the mechanism of cadmium sorption to goethite. Geochim Cosmochim Acta 63(19):2989–3002. https://doi.org/10.1016/S0016-7037(99)00226-4

Cui L, Zhu X, Ma M, Ouyang Y, Dong M, Zhu W, Luo S (2008) Phosphorus sorption capacities and physicochemical properties of nine substrate materials for constructed wetland. Arch Environ Contam Toxicol 55(2):210–217. https://doi.org/10.1007/s00244-007-9109-y

Cusack PB, Callery O, Courtney R, Ujaczki E, O'Donoghue LMT, Healy MG (2019) The use of rapid, small-scale column tests to determine the efficiency of bauxite residue as a low-cost adsorbent in the removal of dissolved reactive phosphorus from agricultural waters. J Environ Manag 241:273–283. https://doi.org/10.1016/j.jenvman.2019.04.042

Delaney P, Mcmanamon C, Hanrahan JP, Copley MP, Holmes JD, Morris MA (2011) Development of chemically engineered porous metal oxides for phosphate removal. J Hazard Mater 185(1):382–391. https://doi.org/10.1016/j.jhazmat.2010.08.128

Drizo A, Forget C, Chapuis RP, Comeau Y (2006) Phosphorus removal by electric arc furnace steel slag and serpentinite. Water Res 40(8):1547–1554. https://doi.org/10.1016/j.watres.2006.02.001

Environmental Protection Agency of China (2002) Environmental quality standard for surface water. China Standard Press, Beijing GB 3838-2002

Fu J, Song R, Mao WJ, Wang Q, An SQ, Zeng QF, Zhu HL (2011) Adsorption of disperse blue 2BLN by microwave activated red mud. Environ Prog Sustain Energy 30(4):558–566. https://doi.org/10.1002/ep.10506

Gan F, Zhou J, Wang H, Du C, Chen X (2009) Removal of phosphate from aqueous solution by thermally treated natural palygorskite. Water Res 43(11):2907–2915. https://doi.org/10.1016/j.watres.2009.03.051

Gao J, Zhao J, Zhang J, Li Q, Gao J, Cai M, Zhang J (2020) Preparation of a new low-cost substrate prepared from drinking water treatment sludge (DWTS)/bentonite/zeolite/fly ash for rapid phosphorus removal in constructed wetlands. J Clean Prod 261:121110. https://doi.org/10.1016/j.jclepro.2020.121110

García J, ROUSSEAU DPL, MORATó J, LESAGE E, MATAMOROS V, BAYONA JM (2010) Contaminant removal processes in subsurface-flow constructed wetlands: a review. Crit Rev Environ Sci Technol 40(7):561–661. https://doi.org/10.1080/10643380802471076

Gustafsson JP, Renman A, Renman G, Poll K (2008) Phosphate removal by mineral-based sorbents used in filters for small-scale wastewater treatment. Water Res 42(1):189–197. https://doi.org/10.1016/j.watres.2007.06.058

Hai NT, You SJ, Hosseini-Bandegharaei A, Chao HP (2017) Mistakes and inconsistencies regarding adsorption of contaminants from aqueous solutions: a critical review. Water Res 120(1):88–116. https://doi.org/10.1016/j.watres.2017.04.014

Han X, Liu Z, Lu T, Gu L, Gu Y (2019) Preparation of modified polyaluminium chloride residue and its phosphorus removal performance. Inorg Chem Ind 51(4):59–62

Jiang Y, Deng T, Yang K, Wang H (2017) Removal performance of phosphate from aqueous solution using a high-capacity sewage sludge-based adsorbent. J Taiwan Inst Chem Eng 76:59–64. https://doi.org/10.1016/j.jtice.2017.04.002

Jie C, Yun C, Malcolm C, Yan Y, Hong J (2013) Equilibrium and kinetic studies of phosphate removal from solution onto a hydrothermally modified oyster shell material. PLoS One 8(4):60243. https://doi.org/10.1371/journal.pone.0060243

Jung KW, Hwang MJ, Ahn KH, Ok YS (2015) Kinetic study on phosphate removal from aqueous solution by biochar derived from peanut shell as renewable adsorptive media. Int J Environ Sci Technol 12(10):3363–3372. https://doi.org/10.1007/s13762-015-0766-5

Kuśmierek K, Szala M, Świątkowski A (2016) Adsorption of 2,4-dichlorophenol and 2,4-dichlorophenoxyacetic acid from aqueous solutions on carbonaceous materials obtained by combustion synthesis. J Taiwan Inst Chem Eng 63:371–378. https://doi.org/10.1016/j.jtice.2016.03.036

Lan W, Zhang J, Hu Z, Ji M, Zhang X, Zhang J, Li F, Yao G (2018) Phosphorus removal enhancement of magnesium modified constructed wetland microcosm and its mechanism study. Chem Eng J 335:209–214. https://doi.org/10.1016/j.cej.2017.10.150

Li M, Liu J, Xu Y, Qian G (2016) Phosphate adsorption on metal oxides and metal hydroxides: a comparative review. Environ Rev 24(3):319–332. https://doi.org/10.1139/er-2015-0080

Lin J, Zhan Y, Wang H, Chu M, Wang C, He Y, Wang X (2017) Effect of calcium ion on phosphate adsorption onto hydrous zirconium oxide. Chem Eng J 309:118–129. https://doi.org/10.1016/j.cej.2016.10.001

Littler J, Geroni JN, Sapsford DJ, Coulton R, Griffiths AJ (2013) Mechanisms of phosphorus removal by cement-bound ochre pellets. Chemosphere 90(4):1533–1538. https://doi.org/10.1016/j.chemosphere.2012.08.054

Liu J, Wan L, Zhang L, Zhou Q (2011) Effect of pH, ionic strength, and temperature on the phosphate adsorption onto lanthanum-doped activated carbon fiber. J Colloid Interface Sci 364(2):490–496. https://doi.org/10.1016/j.jcis.2011.08.067

Liu J, Zhou Q, Chen J, Zhang L, Chang N (2013) Phosphate adsorption on hydroxyl–iron–lanthanum doped activated carbon fiber. Chem Eng J 215:859–867. https://doi.org/10.1016/j.cej.2012.11.067

Liu W, Zhao X, Wang T, Fu J, Ni JR (2015) Selective and irreversible adsorption of mercury(II) from aqueous solution by a flower-like titanate nanomaterial. J Mater Chem 3(34):17676–17684. https://doi.org/10.1039/C5TA04521E

Liu R, Zhao Y, Sibille C, Ren B (2016) Evaluation of natural organic matter release from alum sludge reuse in wastewater treatment and its role in P adsorption. Chem Eng J 302:120–127. https://doi.org/10.1016/j.cej.2016.05.019

Liu R, Chi L, Wang X, Sui Y, Wang Y, Arandiyan H (2018) Review of metal (hydr)oxide and other adsorptive materials for phosphate removal from water. J Environ Chem Eng 6(4):5269–5286. https://doi.org/10.1016/j.jece.2018.08.008

Lu SG, Bai SQ, Zhu L, Shan HD (2009) Removal mechanism of phosphate from aqueous solution by fly ash. J Hazard Mater 161(1):95–101. https://doi.org/10.1016/j.jhazmat.2008.02.123

Ma P, Ding W, Yuan J, Yi L, Zhang H (2020) Total recycle strategy of phosphorus recovery from wastewater using granule chitosan inlaid with γ-AlOOH. Environ Res 184:109309. https://doi.org/10.1016/j.envres.2020.109309

Mitrogiannis D, Psychoyou M, Baziotis I, Inglezakis VJ, Koukouzas N, Tsoukalas N, Palles D, Kamitsos EI, Oikonomou G, Markou G (2017) Removal of phosphate from aqueous solutions by adsorption onto Ca(OH)$_2$ treated natural clinoptilolite. Chem Eng J 320:510–522. https://doi.org/10.1016/j.cej.2017.03.063

Mockler EM, Deakin J, Archbold M, Gill L, Daly D, Bruen M (2017) Sources of nitrogen and phosphorus emissions to Irish rivers and coastal waters: estimates from a nutrient load apportionment framework. Sci Total Environ 601:326–339. https://doi.org/10.1016/j.scitotenv.2017.05.186

Na LI, Hao X, Yijun LU, Jimei C, Dongyun DU (2011) Treatment and utilization of waste residue produced from polyaluminium chloride process. CIESC Journal 62(5):1441–1447. https://doi.org/10.3969/j.issn.0438-1157.2011.05.039

Oguz E (2005) Sorption of phosphate from solid/liquid interface by fly ash. Colloids Surf A Physicochem Eng Asp 262(1-3):113–117. https://doi.org/10.1016/j.colsurfa.2005.04.016

Özer A, Akkaya G, Turabik M (2005) The biosorption of Acid Red 337 and Acid Blue 324 on Enteromorpha prolifera: the application of nonlinear regression analysis to dye biosorption. Chem Eng J 112(1):181–190. https://doi.org/10.1016/j.cej.2005.07.007

Panagiotou E, Kafa N, Koutsokeras L, Kouis P, Nikolaou P, Constantinides G, Vyrides I (2018) Turning calcined waste egg shells and wastewater to brushite: phosphorus adsorption from aqua media and anaerobic sludge leach water. J Clean Prod 178:419–428. https://doi.org/10.1016/j.jclepro.2018.01.014

Pearson RG (1968) Hard and Soft Acids and Base, HSAB, Part I, Fundamental principles. J Chem Educ 45(9):581. https://doi.org/10.1021/ed045p581

Raganati F, Alfe M, Gargiulo V, Chirone R, Ammendola P (2018) Isotherms and thermodynamics of CO$_2$ adsorption on a novel carbon-magnetite composite sorbent. Chem Eng Res Des 134:540–552. https://doi.org/10.1016/j.cherd.2018.04.037

Ruiting L, Lina C, Xinze W, Yanming S, Yuan W, Hamidreza A (2018) Review of metal (hydr)oxide and other adsorptive materials for phosphate removal from water. J Environ Chem Eng 6(4):5269–5286. https://doi.org/10.1016/j.jece.2018.08.008

Su Y, Cui H, Li Q, Gao S, Shang JK (2013) Strong adsorption of phosphate by amorphous zirconium oxide nanoparticles. Water Res 47(14):5018–5026. https://doi.org/10.1016/j.watres.2013.05.044

Tran HN, Lin CC, Woo SH, Chao HP (2018) Efficient removal of copper and lead by Mg/Al layered double hydroxides intercalated with

organic acid anions: adsorption kinetics, isotherms, and thermodynamics. Appl Clay Sci 154:17–27. https://doi.org/10.1016/j.clay.2017.12.033

Vohla C, Koiv M, Bavor HJ, Chazarenc F, Mander, ü. (2011) Filter materials for phosphorus removal from wastewater in treatment wetlands—a review. Ecol Eng 37(1):70–89. https://doi.org/10.1016/j.ecoleng.2009.08.003

Wang S, Kong L, Long J, Su M, Diao Z, Chang X, Chen D, Song G, Shih K (2018) Adsorption of phosphorus by calcium-flour biochar: isotherm, kinetic and transformation studies. Chemosphere 195:666–672. https://doi.org/10.1016/j.chemosphere.2017.12.101

Wang H, Xiao K, Yang J, Yu Z, Yu W, Xu Q, Wu Q, Liang S, Hu J, Hou H (2020) Phosphorus recovery from the liquid phase of anaerobic digestate using biochar derived from iron−rich sludge: a potential phosphorus fertilizer. Water Res 174:115629. https://doi.org/10.1016/j.watres.2020.115629

Weber WJ, Smith EH (1987) Simulation and design models for adsorption processes. Environ Sci Technol 21(11):1040–1050. https://doi.org/10.1021/es00164a002

Wei X, Viadero RC, Bhojappa S (2008) Phosphorus removal by acid mine drainage sludge from secondary effluents of municipal wastewater treatment plants. Water Res 42(13):3275–3284. https://doi.org/10.1016/j.watres.2008.04.005

Wu RSS, Lam KH, Lee JMN, Lau TC (2007) Removal of phosphate from water by a highly selective La(III)-chelex resin. Chemosphere 69(2):289–294. https://doi.org/10.1016/j.chemosphere.2007.04.022

Wu H, Fan J, Zhang J, Ngo HH, Guo W, Liang S, Lv J, Lu S, Wu W, Wu S (2016) Intensified organics and nitrogen removal in the intermittent-aerated constructed wetland using a novel sludge-ceramsite as substrate. Bioresour Technol 210:101–107. https://doi.org/10.1016/j.biortech.2016.01.051

Wu B, Wan J, Zhang Y, Pan B, Lo IMC (2019) Selective phosphate removal from water and wastewater using sorption: process fundamentals and removal mechanisms. Environ Sci Technol 54(1):50–66. https://doi.org/10.1021/acs.est.9b05569

Xie J, Wang Z, Lu S, Wu D, Zhang Z, Kong H (2014) Removal and recovery of phosphate from water by lanthanum hydroxide materials. Chem Eng J 254:163–170. https://doi.org/10.1016/j.cej.2014.05.113

Xiong W, Tong J, Yang Z, Zeng G, Zhou Y, Wang D, Song P, Xu R, Zhang C, Cheng M (2017) Adsorption of phosphate from aqueous solution using iron-zirconium modified activated carbon nanofiber: performance and mechanism. J Colloid Interface Sci 493:17–23. https://doi.org/10.1016/j.jcis.2017.01.024

Xiong J, Zang L, Zha J, Mahmood Q, He Z (2019) Phosphate removal from secondary effluents using coal gangue loaded with zirconium oxide. Sustainability 11(9):2453. https://doi.org/10.3390/su11092453

Yang Y, Zhao Y, Babatunde A, Wang L, Ren Y, Han Y (2006) Characteristics and mechanisms of phosphate adsorption on dewatered alum sludge. Sep Purif Technol 51(2):193–200. https://doi.org/10.1016/j.seppur.2006.01.013

Yang S, Zhao Y, Ding D, Wang Y, Zhang Z (2013) An electrochemically modified novel tablet porous material developed as adsorbent for phosphate removal from aqueous solution. Chem Eng J 220(11):367–374. https://doi.org/10.1016/j.cej.2013.01.067

Yang L, Wei J, Liu Z, Wang J, Wang D (2015) Material prepared from drinking waterworks sludge as adsorbent for ammonium removal from wastewater. Appl Surf Sci 330:228–236. https://doi.org/10.1016/j.apsusc.2015.01.017

Yang Y, Zhao Y, Liu R, Morgan D (2018) Global development of various emerged substrates utilized in constructed wetlands. Bioresour Technol 261:441–452. https://doi.org/10.1016/j.biortech.2018.03.085

Yin H, Han M, Tang W (2016) Phosphorus sorption and supply from eutrophic lake sediment amended with thermally-treated calcium-rich attapulgite and a safety evaluation. Chem Eng J 285:671–678. https://doi.org/10.1016/j.cej.2015.10.038

Yu Y, Wu R, Clark M (2010) Phosphate removal by hydrothermally modified fumed silica and pulverized oyster shell. J Colloid Interface Sci 350(2):538–543. https://doi.org/10.1016/j.jcis.2010.06.033

Zhang R, Leiviskä T (2020) Surface modification of pine bark with quaternary ammonium groups and its use for vanadium removal. Chem Eng J 385:123967. https://doi.org/10.1016/j.cej.2019.123967

Zhang J, Shen Z, Mei Z, Li S, Wang W (2011) Removal of phosphate by Fe-coordinated amino-functionalized 3D mesoporous silicates hybrid materials. J Environ Sci 23(2):199–205. https://doi.org/10.1016/S1001-0742(10)60393-2

Zhang H, Chen W, Zhao B, Phillips LA, Zhou Y, Lapen DR, Liu J (2020) Sandy soils amended with bentonite induced changes in soil microbiota and fungistasis in maize fields. Appl Soil Ecol 146:103378. https://doi.org/10.1016/j.apsoil.2019.103378